Viscoelastic Properties of Hydrocarbon/Fluorocarbon Mixed Wormlike Micelles at High Ionic Strength

E. Buhler,*,† C. Oelschlaeger,‡ G. Waton,‡ and S. J. Candau‡

Groupe de Dynamique des Phases Condensées, UMR No. 5581 CNRS, Université de Montpellier II, Case Courrier 26, Place Eugène Bataillon, 34095 Montpellier Cedex 5, France, and Laboratoire de Dynamique des Fluides Complexes, UMR No. 7506 CNRS, Université Louis Pasteur, 4, rue Blaise Pascal, 67070 Strasbourg Cedex, France.

Received: February 5, 2004; In Final Form: May 17, 2004

The mixed micellization between the perfluorooctylbutane trimethylammonium bromide (C_8F_{17}) and the cetyltrimethylammonium bromide (CTAB) surfactants in the presence of KBr has been investigated. Surface tension experiments revealed a demixed micelles behavior. At high ionic strength ([KBr] ≥ 100 mM), semidilute solutions exhibit a phase separation between vesicles and micelles when the molar ratio $R = [C_8F_{17}]/([C_8F_{17}] + [\text{CTAB}])$ exceeds ∼0.3. In the monophasic domain, light scattering and *T*-jump experiments performed on the dilute regime as well as measurements by dynamic light scattering of the terminal viscoelastic relaxation time in the semidilute range suggest a continuous micellar growth as *R* increases. At lower ionic strength ([KBr] = 30 mM), the systems remain monophasic in the whole *R* range. The terminal relaxation time increases continuously with *R*, the increase becoming very steep in the vicinity of $R = 1$, which strongly suggests a structural transition within the micellar aggregates.

1. Introduction

Mixed surfactant systems have been widely studied over the past two decades.[1−3] Synergistic micellization as well as formation of partially mixed systems more or less rich in one surfactant were reported.[4−19] In a previous study, the mixed micellization of dimeric and single-hydrocarbon chain cationic surfactant solutions at high ionic strength has been investigated (i.e., mixtures of gemini ethan-diyl-1,2-bis(dodecyldimethylammonium bromide) hereafter called 12-2-12 and cetyltrimethylammonium bromide hereafter called CTAB).[20] The variation of the cmc (critical micelle concentration) of the mixtures with composition revealed synergism in micelle formation. Moreover, rheology and light scattering measurements revealed synergistic gains in viscoelastic properties with a maximum of the stress-relaxation time around the equimolar composition. These effects were ascribed to a progressive intermicellar cross-linking resulting from a continuous increase of the end-cap energy with the gemini (dimeric surfactant) content in the mixture.

In this paper we are interested in the behavior of mixtures of two surfactants with incompatible fluorocarbon and hydrocarbon hydrophobic moieties. In this case, one expects the formation of two micellar populations, i.e., micelles mainly composed of fluorocarbon surfactants in equilibrium with micelles mainly composed of hydrocarbon surfactants. For the purpose of this study, we have selected the perfluorooctylbutane trimethylammonium bromide hereafter called C_8F_{17} and the cetyltrimethylammonium bromide (CTAB). Up to now, most of the studies on this type of system were carried out in the vicinity of the critical micelle concentration (cmc). We have studied the structure, the kinetics, and the dynamics of mixtures at high ionic strength under conditions where the micelles are expected to adopt a cylindrical shape. In the low concentration range, surface tension measurements were performed to determine the mixed critical micelle concentration. In the dilute regime and in the vicinity of the overlap micellar volume fraction ϕ^*, we have studied both kinetic and structural properties of surfactant mixtures through *T*-jump and light scattering experiments, respectively. Finally, the viscoelastic properties were investigated in the semidilute regime by means of light scattering.

This study was mostly focused on the effect of the end-cap energy on the structural and dynamical properties of these mixed systems. The end-cap energy increases with the C_8F_{17} in the mixture, because for [KBr] > 30 mM the C_8F_{17} self-assembles into vesicles,[21] whereas the CTAB forms cylindrical micelles.[20] However, the incompatibility between surfactants might also induce a micellar segregation, which could confer specific properties to the systems. Mixtures of C_8F_{17} and CTAB have been investigated in the presence of 100 mM KBr in the dilute regime and in the presence of 200, 100, or 30 mM KBr in the semidilute regime.

2. Materials and Methods

2.1. Materials. The perfluorooctylbutane trimethylammonium bromide [$C_8F_{17}(CH_2)_4N^+(CH_3)_3Br^-$ ($M = 614$ g/mol)] surfactant (C_8F_{17}) has been synthesized using a method involving four steps, as previously reported.[21] Cetyltrimethylammonium bromide (CTAB) was obtained from Acros Organics. The solutions were prepared by weighting the components. As both surfactants have a density close to one, we will take in the following the weight concentration equal to the volume fraction ϕ.

2.2. Surface Tension Measurements. The equilibrium surface tensions of the aqueous surfactant solutions were measured with a Lauda tensiometer at $T = 30$ °C using the du Nouy ring method. Sets of measurements were taken at 30 min

* Corresponding author. E-mail: buhler@gdpc.univ-montp2.fr. Phone: +33 (0)4 67 14 39 82. Fax: +33 (0)4 67 14 46 37.
† Université de Montpellier II.
‡ Université Louis Pasteur.

10.1021/jp049466k CCC: $27.50
Published on Web 06/25/2004

intervals until no significant change occurred. The precision of the surface tension measurements is 0.2 mN/m.

2.3. *T*-Jump Device. The *T*-jump device has been described elsewhere.[22,23] For *T*-jump measurements the surfactant solutions were filtered through a 0.22 μm Millipore filter. The *T*-jump is produced by means of a discharge of a capacitor through the sample. The rise time of the *T*-jump is 1 μs and its amplitude, calculated from the values of the stored electrical energy and the heat capacity of the sample, can be varied between 0.1 and 2 °C. The scattering cell is illuminated by an intense light beam obtained from a powerful (150 W) mercury xenon lamp in conjunction with a large-aperture condenser (ORIEL Aspherab). Several interference filters allow for the selection of the following wavelengths: 313, 365, 405, 436, 546, and 577 nm. A fraction of the incident light beam is sent to the photodiode, which thus delivers a reference signal. An electronic device uses this signal to compensate lamp power or arc position instabilities.

Two photomultipliers (PM) are used for the detection of the light scattered at 90° and 20° angles. A photodiode placed on the optical axis measures the transmitted light.

The PM signal is digitalized and acquired using a pseudologarithmic time-base in which the sampling time is periodically increased. For each measurement, several relaxation functions are summed up to get an averaged curve. This results in a further improvement of the signal/noise ratio. After the *T*-jump, the temperature in the cell decreases slowly and it may be considered as constant during 5 s. The temperature in the cell is controlled to ±0.1 °C.

2.4. Light Scattering Experiments. Static light scattering (SLS) and dynamic light scattering (DLS) experiments were performed by means of a spectrometer equipped with an argon ion laser (Spectra Physics model 2020) operating at $\lambda = 488$ nm, an ALV-5000 correlator (ALV, Langen-Germany Instruments), a computer-controlled and stepping-motor-driven variable angle detection system, and a temperature-controlled sample cell. The scattering spectrum was measured through a band-pass filter (488 nm) and a pinhole (200 μm for the static experiments and 100 or 50 μm for the dynamic experiments) with a photomultiplier tube (ALV).[24]

In the SLS experiments, the excess of scattered intensity $I(q)$ was measured with respect to the solvent, where the magnitude of the scattering wave vector q is given by

$$q = \frac{4\pi n}{\lambda} \sin\frac{\theta}{2} \tag{1}$$

In eq 1, n is the refractive index of the solvent (1.34 for the water at 25 °C), λ is the wavelength of light in the vacuum, and θ is the scattering angle. In our experiments, the scattering angle θ was varied between 20° and 150°, which corresponds to scattering wave vectors q in the range from 6×10^{-4} to 3.2×10^{-3} Å^{-1}. The absolute scattering intensities $I(q)$ (i.e., the excess Rayleigh ratios) were deduced by using a toluene sample reference for which the excess Rayleigh ratio is well-known, i.e., 40×10^{-6} cm^{-1} at 488 nm.[25]

In the dynamic light scattering experiments (DLS), the normalized time autocorrelation function $g^{(2)}(q,t)$ of the scattered intensity is measured.[25]

$$g^{(2)}(q,t) = \frac{\langle I(q,0)\, I(q,t)\rangle}{\langle I(q,0)\rangle^2} \tag{2}$$

The latter can be expressed in terms of the field autocorrelation function or equivalently in terms of the autocorrelation function of the concentration fluctuations $g^{(1)}(q,t)$ through

$$g^{(2)}(q,t) = A + \beta|g^{(1)}(q,t)|^2 \tag{3}$$

where A is the baseline and β is the coherence factor, which in our experiments is equal to 0.7−0.9. The normalized dynamical correlation function $g^{(1)}(q,t)$ of polymer concentration fluctuations is defined as

$$g^{(1)}(q,t) = \frac{\langle \delta c(q,0)\, \delta c(q,t)\rangle}{\langle \delta c(q,0)^2\rangle} \tag{4}$$

where $\delta c(q,t)$ and $\delta c(q,0)$ represent fluctuations of polymer concentration at time t and zero, respectively.

In the dilute regime, the time decay of $g^{(1)}(q,t)$ is a single exponential with a characteristic time inversely proportioned to q^2, which characterizes a diffusive behavior. For these solutions we have adopted the classical cumulant analysis.[26] This analysis provides the variance of the correlation function and the first reduced cumulant $(\tau q^2)^{-1}$, where τ is the average relaxation time of $g^{(1)}(q,t)$. The extrapolation of $(\tau q^2)^{-1}$ to $q = 0$ yields the values of the mutual diffusion constant D. The latter is related to the average hydrodynamic radius R_H of the micelles through

$$D = \frac{kT}{6\pi\eta_s R_H} = \left(\frac{1}{\tau q^2}\right)_{q^2=0} \tag{5}$$

where k is the Boltzman constant, η_s the solvent viscosity, and T the absolute temperature.

We also used another method to determine the average relaxation time τ: the Contin method based on the inverse Laplace transform of $g^{(1)}(q,t)$.[27] If the spectral profile of the scattered light can be described by a multi-Lorentzian curve, then $g^{(1)}(q,t)$ can be written as

$$g^{(1)}(q,t) = \int_0^\infty G(\Gamma) \exp(-\Gamma t)\, d\Gamma \tag{6}$$

where $G(\Gamma)$ is the normalized decay constant distribution. This method is more appropriate for the solutions characterized by several relaxations mechanisms (semidilute regime).

3. Results and Discussion

3.1. Surface Tension Properties in the Vicinity of the cmc. The variations of the surface tension with the logarithm of the overall surfactant concentration are reported in Figure 1 for various C_8F_{17}/CTAB mixtures. For both pure surfactant solutions, these variations present a single change in the slope at the critical micelle concentration, cmc. The latter is found to be equal to 3.5×10^{-5} and to 10^{-4} M for the C_8F_{17} and CTAB surfactants, respectively (see Figure 1a). As shown in Figure 1b, the same behavior is observed for mixtures with values of the molar ratio $R = [C_8F_{17}]/([CTAB] + [C_8F_{17}])$ equal to 0.26 and to 0.6 and with values of the cmc respectively equal to 2×10^{-4} and 10^{-4} M. However, for the equimolar mixture of C_8F_{17} and CTAB the shape of the curve represented in Figure 1c and describing the variation of the surface tension with the total surfactant concentration is different. Indeed for $R = 0.5$, one can determine two slope changes in the curve, corresponding to two different cmc values: $cmc_1 \sim 5 \times 10^{-5}$ M and $cmc_2 \sim 4 \times 10^{-4}$ M. From the results described above, the following comments can be made: (i) The addition of a moderate fluorocarbon surfactant quantity ($R = 0.26$) is sufficient to lower the surface tension at the plateau to a value close to that of the pure fluorocarbon surfactant. In this case, only one cmc ($\sim 2 \times 10^{-4}$ M) larger than that of both surfactants can be determined.

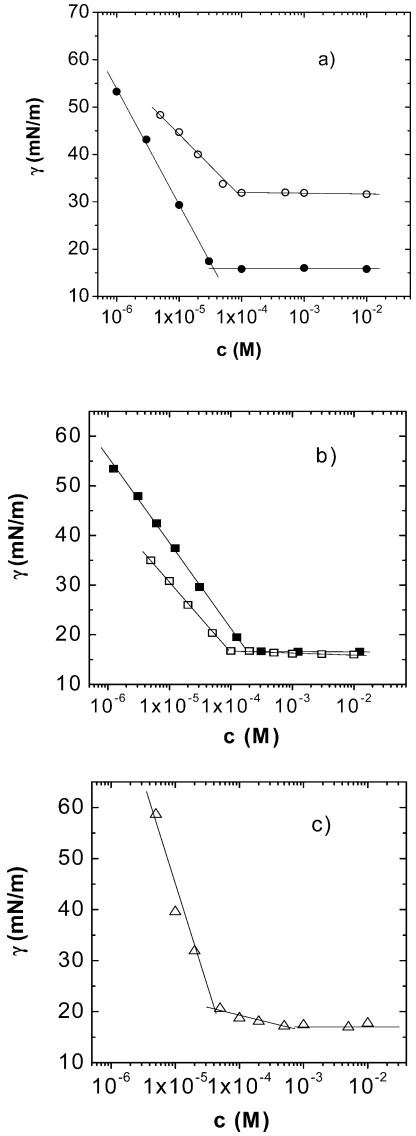

Figure 1. Variation of the surface tension as a function of the logarithm of the overall surfactant concentration, $T = 30$ °C, [KBr] = 100 mM. (a) (○) CTAB, (●) C_8F_{17}; (b) (■) $R = 0.26$, (□) $R = 0.6$; (c) (△) $R = 0.5$. Experimental error is equal to 5%.

This behavior is characteristic of incompatible surfactants and of a tendency to the formation of demixed micelles. The parameter of interaction, β, can be extracted from the equations derived for nonideal mixture of surfactants:[28]

$$\frac{x^2 \log(X\mathrm{cmc_M}/x\mathrm{cmc_F})}{(1-x^2)\log[(1-X)\mathrm{cmc_M}/(1-x)\mathrm{cmc_F}]} = 1 \qquad (7)$$

and

$$\beta = \left[\log \frac{X\,\mathrm{cmc_M}}{x\,\mathrm{cmc_F}}\right]/(1-x)^2 \qquad (8)$$

where X and x are the mole fractions of fluorocarbon surfactant in the mixture and in the micelles, respectively, $\mathrm{cmc_F}$ is the cmc of C_8F_{17} and $\mathrm{cmc_M}$ that of the mixture of composition X. If $\beta \geq 2$, demixed micelles should form, due to the repulsive force between surfactants.[9,13,28−33] In the present case ($R = 0.26$), β is found to be equal to 6.13. If $\beta = 0$, an ideal mixing behavior is expected whereas negative interaction parameters indicate attractive interactions in mixed micellization. However, the

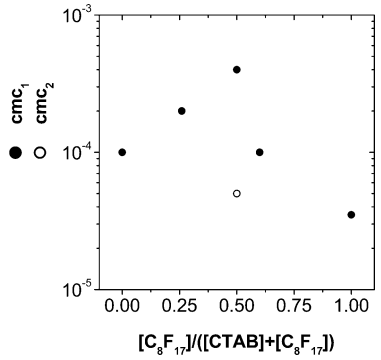

Figure 2. Variation of the critical micelles concentrations, cmc, deduced from Figure 1 as a function of the molar ratio $R = [C_8F_{17}]/([\mathrm{CTAB}] + [C_8F_{17}])$, $T = 30$ °C, [KBr] = 100 mM.

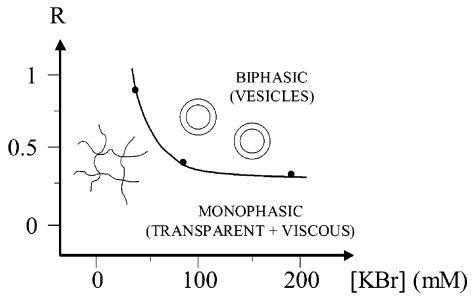

Figure 3. Partial phase diagram of mixed C_8F_{17}/CTAB; $\phi_T = 8 \times 10^{-2}$, $T = 35$ °C.

variation of the surface tension observed in Figure 1b for $R = 0.26$ rather suggests the presence of a single micelle population of surfactant composition similar to that of the mixture. We will see in the following parts that the light scattering and T-jump results support such an explanation. (ii) The behavior described above for the equimolar surfactant mixture was often observed in other systems and was attributed to the existence of two different cmc.[9,14] One can safely assume that the first cmc (close to that of pure C_8F_{17}) corresponds to the formation of micelles mainly composed of fluorocarbon surfactants whereas the second one (larger than that of CTAB) characterizes the formation of micelles mainly composed of CTAB. One should note the low amplitude of the decay between the two cmc. (iii) The latter remark could explain the results obtained with the $R = 0.6$ sample where we observe only one cmc, which could be ascribed to the first one; the second one being undetectable due to a too low variation of the surface tension and a too low gap between the two cmc. For this system, the analysis of the data using eqs 7 and 8 leads to a value of β equal to 4, in favor of a demixed micelles behavior. In Figure 2 are depicted the variations of the cmc as a function of the mixture composition.

3.2. Partial Phase Diagram of the System C_8F_{17}/CTAB. We have determined the partial phase diagram of mixtures of C_8F_{17} and CTAB for a total surfactant volume fraction, $\phi_T = 8 \times 10^{-2}$, much larger than the overlap concentration, as a function of the molar ratio $R = [C_8F_{17}]/([\mathrm{CTAB}] + [C_8F_{17}])$ and of the excess KBr salt concentration at fixed temperature $T = 35$ °C. The determination was made visually, the entangled micellar solutions being transparent and highly viscous. Figure 3 summarizes the observations. For low salt contents ([KBr] < 50 mM), the solutions are monophasic, transparent and viscous over the whole range of molar ratio whereas they are monophasic only for $R \leq 0.31$ at higher salt concentrations ([KBr] ≥ 200 mM). For [KBr] ≥ 50 mM, upon increasing the molar ratio to $R > 0.31$, one observes a phase separation between a turbid

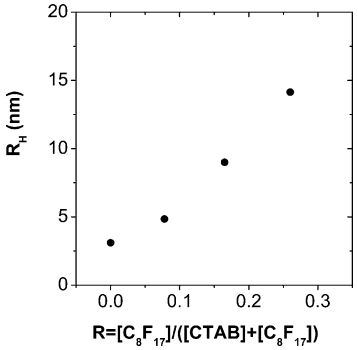

Figure 4. Molar ratio R dependence of the hydrodynamic radius in the dilute regime, $T = 35$ °C, $\phi_T = 4 \times 10^{-3}$, [KBr] = 100 mM. Experimental error is equal to 5%.

solution and a transparent and viscous phase. Optical microscopy observations of the turbid phase show the presence of polydisperse vesicles, with diameters about 10 μm. As explained above, these two surfactants show separately a tendency to form self-assemblies with different curvatures, the CTAB forming wormlike micelles whereas the C_8F_{17} self-assembling into vesicles. Thus, the transparent and viscous phase corresponds to the formation of entangled wormlike micelles mainly composed of CTAB whereas the turbid phase corresponds to the formation of vesicles mainly composed of fluorocarbon surfactants.

3.3. Kinetics and Structure of Micelles in the Dilute Regime. *3.3.1. Light Scattering Experiments.* Dynamic light scattering experiments were performed on dilute solutions ($\phi = 4 \times 10^{-3}$) of C_8F_{17}/CTAB mixtures with R successively equal to 0, 0.078, 0.165, and 0.26 and $T = 35$ °C. In all cases, the normalized field autocorrelation function, $g^{(1)}(q,t)$, is characterized by a single exponential relaxation function. The peak in the time distribution function obtained using the classical Contin method is symmetrical and quite narrow, as expected for a simple exponential decay. The cumulant analysis provides a variance of the correlation function close to 0.2 at low scattering angles for the four investigated mixtures. Furthermore, the angular dependence shows that this relaxation is diffusive with a characteristic time inversely proportioned to q^2. These results suggest the presence of a single micelle population for which we can calculate a diffusion coefficient for each mixture. In Figure 4 is presented the variation of the average hydrodynamic radius R_H obtained using the Stokes−Einstein relation with the fluorocarbon surfactant content. As the proportion of the fluorocarbon surfactant increases, a progressive increase of the micelle hydrodynamic radius is also observed. Indeed, R_H is equal to 3 nm for pure CTAB solutions whereas it reaches a value of 15 nm for the composition $R = 0.26$. A continuous increase of the micellar mean length with the molar ratio is characteristic of an increase of the end-cap energy as one incorporates fluorocarbon surfactants into the CTAB micelles. Let us recall that the system phase separates for $R \geq 0.31$.

3.3.2. T-Jump Experiments. T-jump experiments are ideally suited to study the kinetics of dilute solutions or solutions in the vicinity of the overlap concentration ϕ^* where the signal is sensitive to a change in the micellar length distribution induced by a change of temperature.[22,23] For a system of linear micelles undergoing a reversible breakdown process, the micellar length distribution is predicted to decay monoexponentially with a relaxation time $\tau_{T-J} = \tau_{break}/2$, where τ_{break} is the time taken for a micelle of the mean length to break, inversely proportional to the average micellar length $\bar{L}$.[34,35] For all the C_8F_{17}/CTAB aqueous solutions, the T-jump responses are well described by a single-exponential decay. As shown in Figure 5a, and except

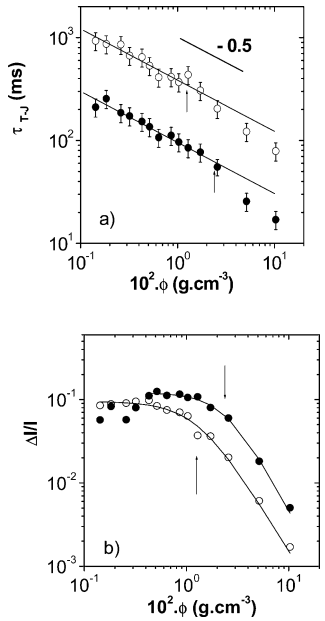

Figure 5. Variation of the characteristic time τ_{T-J} (a) and of the amplitudes (b) as a function of the overall surfactant volume fraction. [KBr] = 100 mM, $R = 0.26$, and $T = 35$ °C (○) or $T = 45$ °C (●). Arrows indicate the critical overlap concentrations determined from the fits of the amplitudes (black lines) using eq 9.

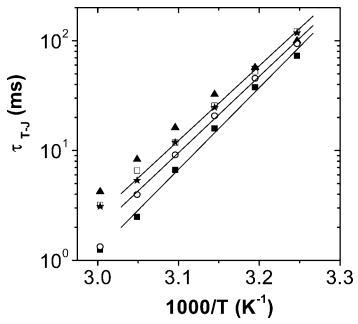

Figure 6. Dependence of the characteristic times τ_{T-J} on the temperature for various mixtures of C_8F_{17} and CTAB. [CTAB] = 100 mM, [KBr] = 100 mM, and [C_8F_{17}] = 0 mM (■), 4.88 mM (○), 12.2 mM (★), 24.43 mM (□), and 48.86 mM (▲).

for the higher concentrations where amplitudes become very low, the relaxation time τ_{T-J} scales with the total surfactant volume fraction with an exponent of about −0.5 over a wide range of concentrations. Such a value for the exponent is in agreement with the theoretically predicted $\phi^{0.5}$ dependence of the average length $\bar{L}$ for single population solutions of linear micelles.[34,35] Typical variations of the amplitude of the relative scattering decrease, induced by the T-jump, with the total surfactant volume fraction are presented in Figure 5b for [KBr] = 100 mM and $R = 0.26$. The arrows represented in Figure 5a,b represent the critical overlap volume fraction ϕ^* determined using the following relationship derived for solutions of wormlike micelles:[23]

$$\frac{\Delta I}{I} \approx \frac{1}{1 + 0.95\left(\frac{\phi}{\phi^*}\right)^{1.64}} \qquad (9)$$

The effect of the addition of the fluorocarbon surfactant into the CTAB micelles, at a given temperature, can be observed in Figure 6. The increase of the characteristic relaxation time upon increasing the C_8F_{17} content (see Table 1 for R values) in a CTAB solution of constant concentration equal to 100 mM

TABLE 1: Effect of the Addition of C_8F_{17} on the Energies of Activation E_{break}; [KBr] = 100 mM and [CTAB] = 100 mM

$[C_8F_{17}]$ (mM)	R	E_{break} (kT)
0	0	57
4.88	0.047	53
12.2	0.109	51
24.43	0.196	49
48.86	0.33	46

cannot be explained by the increase of the length of the linear chains revealed by the dynamic light scattering experiments because the time τ_{T-J} associated with the scission-recombination process varies like[36]

$$\tau_{T-J} \approx \frac{1}{k_1 \bar{L}} \tag{10}$$

where k_1 is a rate constant. Also the variation of concentration resulting from the addition of C_8F_{17} into the CTAB solution leads to a decrease in τ_{T-J}. Thus, we can conclude that the scission rate constant k_1 of micelles decreases upon increasing the C_8F_{17} content. The semilog plots of the characteristic relaxation time as a function of $10^3/T$ are described by straight lines, which indicates a typical Arrhenius behavior (see Figure 6). Energies of activation E_{break} associated with $\tau_{break} \sim \tau_{T-J}$ and deduced from the slopes of these lines are collected in Table 1. These values are comparable to those observed for other systems.[20] We can, however, observe a slight decrease of E_{break} when the C_8F_{17} content is increasing, which could be attributed to the repulsive energy between the two surfactants (cf. surface tension measurements).

3.4. Viscoelastic Properties in the Semidilute Regime. The linear viscoelasticity of wormlike micelles, which is classically investigated by means of rheological experiments, can also be studied by dynamic light scattering (DLS).[20,37−40] In particular, DLS provides measurements of the terminal time of the stress relaxation T_R. When $\tau_{break} \ll \tau_{rep}$, where τ_{rep} is the reptation time, the stress relaxation function is a single exponential and $T_R = (\tau_{rep}\tau_{break})^{1/2}$. In this study we have used the DLS technique as it allows us to save surfactant product because the amount of surfactant required for such experiment is about 8 times less than for a rheological measurement.

We have investigated the effect of the composition of semidilute solutions of C_8F_{17}/CTAB mixtures on the terminal time and elastic moduli for two different ionic strengths.

3.4.1. Behavior at High Ionic Strength. In this part, we have studied mixtures of entangled linear micelles at a total surfactant volume fraction, $\phi_T = 8 \times 10^{-2}$, much larger than the overlap concentration in the presence of 200 mM KBr for various compositions: $R = 0.078$, 0.166, and 0.26, a phase separation appearing at $R = 0.31$. Figure 7 shows a typical scattered electric field autocorrelation function, $g^{(1)}(q,t)$, obtained at different scattering wave vectors q and for a molar ratio $R = 0.078$. The DLS results show two well-defined characteristic times for the relaxation function $g^{(1)}(q,t)$. Inspection of Figure 8a,b, representing the variations of $1/\tau_{fast}q^2$ and τ_{slow} with q^2, respectively, shows clearly that the fast mode is diffusive with a characteristic time τ_{fast} inversely proportioned to q^2 whereas the slow relaxation time τ_{slow} is independent of the scattering vector. The relative amplitudes of the slow and fast modes, A_{fast} and A_{slow}, are also independent of q within the experimental accuracy. From the fast relaxation time one obtains the collective diffusion coefficient D_g associated with the gellike fluctuations of the system. It is important to note that D_g is roughly independent

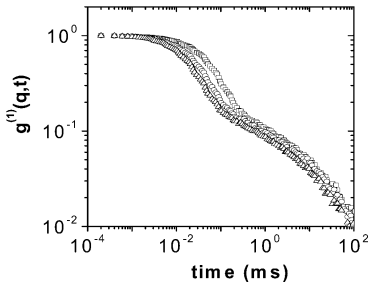

Figure 7. Time autocorrelation function of the scattered electric field for different scattering angles for an aqueous solution of a surfactant mixture. $R = 0.078$, $\phi_T = 8 \times 10^{-2}$, $T = 30$ °C, [KBr] = 200 mM. (□) $q = 1.7 \times 10^{-2}$ nm^{-1}, (○) $q = 2.44 \times 10^{-2}$ nm^{-1}, and (△) $q = 3 \times 10^{-2}$ nm^{-1}.

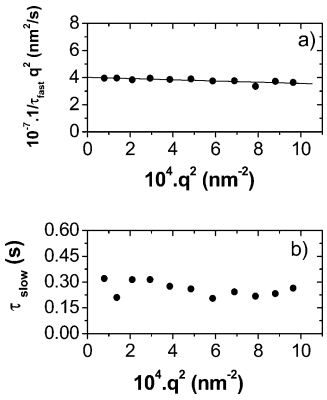

Figure 8. Variations of the ratio $1/\tau_{fast}q^2$ (a) and of the characteristic slow relaxation time (b) with q^2 measured in a $\phi_T = 8 \times 10^{-2}$ semidilute solution. $R = 0.26$, $T = 30$ °C, and [KBr] = 200 mM.

of the composition whereas τ_{slow} exhibits a large increase with the molar ratio R (cf. Table 2a).

The q-independent viscoelastic slow mode was observed in many other systems[20,37−40] and was first predicted by Brochard and de Gennes for semidilute polymer solutions in theta solvent.[41,42] Actually, two relaxation modes were predicted in their model: (i) A fast gel mode with a characteristic time

$$\tau_{fast} = (D_g q^2)^{-1} = \left[\frac{K_{os}}{M_g + K_{os}}\right](D_c q^2)^{-1} \tag{11}$$

where K_{os} is the osmotic modulus, M_g is the longitudinal modulus of the transient network, and D_c is the collective diffusion coefficient of the liquidlike system. (ii) A slow hydrodynamic mode arising from the coupling between stress and concentration fluctuations characterized by a time

$$\tau_{slow} \approx \tau_{rep}\frac{M_g + K_{os}}{K_{os}} \tag{12}$$

where τ_{rep} is the longest time of conformational relaxation (which is just the reptation time in the case of linear polymers) and is q-independent. The relative amplitude of the slow mode is also q-independent and is given by

$$A_{slow} = \frac{M_g}{M_g + K_{os}} \tag{13}$$

Later on, several other theoretical studies were published on this subject.[43−45] In particular, Semenov has predicted three stages of relaxation of concentration fluctuations in polymer solutions.[43] The first stage is due to the cooperative deformation

TABLE 2: Effect of the Molar Ratio (R) on Parameters Determined from DLS

(a) $R = [C_8F_{17}]/([CTAB] + [C_8F_{17}])$; $\phi = 8 \times 10^{-2}$, $T = 30$ °C, and [KBr] = 200 mM

R	D_g (nm^2/s)	$I(q^2=0)$ (cm^{-1})	A_{fast}	τ_{slow} (ms)	A_{slow}	K_{os} (Pa)	M_g (Pa)
0.078	4.34×10^7	2.53×10^{-3}	0.93	15	0.07	2856	215
0.166	4.1×10^7	2.09×10^{-3}	0.925	50	0.075	3457	280
0.26	4.02×10^7	2.04×10^{-3}	0.87	250	0.13	3542	529

(b) $R = [C_8F_{17}]/([CTAB] + [C_8F_{17}])$; $\phi = 8 \times 10^{-2}$, $T = 30$ °C, and [KBr] = 100 mM

R	D_g (nm^2/s)	$I(q^2=0)$ (cm^{-1})	A_{fast}	τ_{slow} (ms)	A_{slow}	K_{os} (Pa)	M_g (Pa)
0.26	5.2×10^7	2.09×10^{-3}	0.93	10	0.07	3457	260

(c) $\phi = 5 \times 10^{-2}$, $T = 30$ °C, and [KBr] = 30 mM

R	D_g (nm^2/s)	$I(q^2=0)$ (cm^{-1})	A_{fast}	τ_{int} (ms)	A_{int}	τ_{slow} (ms)	A_{slow}	K_{os} (Pa)	M_g (Pa)
0.165	1.02×10^8	5×10^{-4}	0.83			0.1	0.17	5644	1156
0.372	7.91×10^7	4.6×10^{-4}	0.87			0.25	0.13	6135	917
0.64	5.52×10^7	4.4×10^{-4}	0.92			1	0.08	6414	558
0.8	5.16×10^7	2.9×10^{-4}	0.92			42.5	0.08	9753	848
0.9	4.68×10^7	3×10^{-4}	0.95			60	0.05	9390	494
1	3.38×10^7	7.1×10^{-4}	0.59	11.7	0.22	2300	0.19	3975	1280

of entanglement network and is characterized by a time τ_{fast} given by eq 11, the second stage is a Rouse-type relaxation of the macromolecular tension along the tube, and the last stage is associated with the reptation process. The amplitude of the Rouse mode is rather small and the corresponding characteristic time is between τ_{fast} and τ_{slow}. Generally, this mode is undetectable in the DLS experiments. Also, we have shown in previous experimental studies performed on semidilute wormlike solutions[20,38,40] that τ_{slow} corresponds to the terminal time T_R, which depends in the limit $\tau_{break} < \tau_{rep}$ on both the reptation time τ_{rep} and the breaking time τ_{break}.[36,46,47]

The values of D_g, τ_{slow}, A_{slow}, A_{fast}, K_{os}, and M_g obtained for samples with total volume fraction $\phi = 8 \times 10^{-2}$ at $T = 30$ °C and for different values of the molar ratio R (with $R < 0.31$; i.e., below the phase separation) are reported in Table 2a. In Table 2b are given the values of these parameters for a sample at $R = 0.26$ with 100 mM KBr. The osmotic modulus K_{os} was deduced from the absolute scattered intensity at zero-angle, $I(q^2=0)$, using the following relationship:

$$I(q^2 \to 0)\ (\mathrm{cm}^{-1}) = 4\pi^2 n^2 \left(\frac{\delta n}{\delta \phi}\right)^2 \lambda^{-4} \phi^2 K_{os}^{-1} kT \qquad (14)$$

where the refractive index increment of the solution $\delta n/\delta\phi$ was found to be independent of the composition and equal to 0.147 cm^3/g. The values of M_g were then inferred from values of K_{os} and of the characteristic ratio A_{slow}/A_{fast} using the following relation:[38]

$$M_g = K_{os} \frac{A_{slow}}{A_{fast}} \qquad (15)$$

The increase of the terminal relaxation time τ_{slow} with R confirms the previous light scattering results in the dilute regime, showing that the addition of C_8F_{17} induces a micellar growth, because $\tau_{rep} \sim \bar{L}^3$.[46,47] One should, however, note that the increase of the characteristic time $\tau_{T-J} \sim \tau_{break}$ with the C_8F_{17} content, shown in Figure 6, can also contribute to the increase of τ_{slow}. The osmotic modulus K_{os} is almost independent of R, whereas M_g increases significantly with R. Also, the terminal relaxation time increases considerably with the KBr content (cf. Table 2).

The overall behavior, summarized in Table 2a, is quite similar to that observed in the same range of R for mixtures of the two compatible surfactants CTAB and 12-2-12. In the latter case the results were interpreted by assuming that the increase of the end-cap energy, resulting from the addition of 12-2-12, leads first to a micellar growth, then to an intermicellar branching. As a result, the slow relaxation time goes through a maximum, whereas the intermicellar branching produced a continuous increase of M_g and of the plateau modulus G'_∞. In the present case, where the two surfactants are mutually incompatible, the end-cap energy cannot be increased continuously because there is a limited incorporation of the fluorocarbon surfactant into the micelles and the system phase separates beyond $R = 0.31$.

To study mixtures over the whole domain of R, we have performed DLS experiments in the presence of 30 mM KBr, i.e., at an excess salt concentration where R can be varied from 0 to 1 without crossing a phase separation.

3.4.2. Behavior in the Presence of 30 mM KBr. In this part, dynamic light scattering experiments were performed on mixtures of entangled linear micelles at a total volume fraction $\phi = 5 \times 10^{-2}$ and in the presence of 30 mM KBr for various compositions: $R = 0$, 0.165, 0.372, 0.64, 0.8, 0.9, and 1. For the pure CTAB solution, i.e., when $R = 0$, the dynamical structure factor is described by a single-exponential relaxation. One should, however, note that the pure CTAB solution is dilute at $T = 30$ °C.[23] At the opposite, for $R = 1$, the scattered electric field autocorrelation function $g^{(1)}(q,t)$ exhibits three widely time separated relaxation processes, as illustrated in Figure 9a. The distribution function of decay times obtained using the Contin method is presented in Figure 9b. The analysis of Figure 10 representing the variation of the three characteristic relaxation times with q shows that the fast mode is diffusive with a characteristic time τ_{fast} inversely proportioned to q^2 whereas intermediate and slow characteristic times, τ_{int} and τ_{slow}, as well as the corresponding amplitudes are independent of q. The observed behavior is qualitatively that predicted for entangled polymer solutions but the amplitude of the intermediate mode, which is assigned to the Rouse mode, is surprisingly large, of the order of magnitude of that of the slow reptational mode, whereas the theory predicts that it should be about 5 times smaller.[43] Up to now, no observation of this Rouse mode has been reported for other wormlike micelle systems. It must be noted that recent CryoTEM pictures have shown that the C_8F_{17} surfactant, both in salt-free conditions and in the presence of small amount of salt does not form cylindrical micelles but self-assembles into narrow ribbons (5.8 nm/2.3 nm) with a small width polydispersity.[48] Also, the sample investigated here exhibits a very large viscosity that cannot be easily measured by the classical rheological setups. No theoretical treatments of the dynamics of concentration fluctuations for solutions of

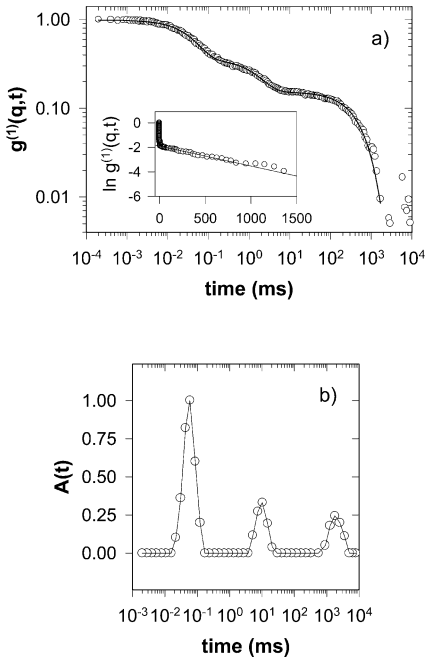

Figure 9. (a) Typical log−log representation of $g^{(1)}(q,t)$ for $\theta = 100°$ relative to a $\phi_T = 5 \times 10^{-2}$ pure C_8F_{17} semidilute solution at temperature $T = 30$ °C and for [KBr] = 30 mM, i.e., $R = 1$. The inset represents $g^{(1)}(q,t)$ in semilog scales and the black line represents the fit of the data in the long time scale. (b) Corresponding distribution function of decay times obtained using the Contin method.

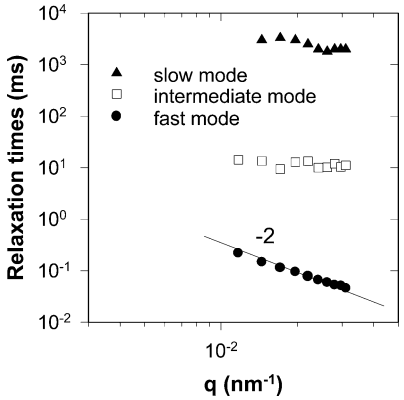

Figure 10. Variation of the fast characteristic time, of the intermediate characteristic time and of the slow characteristic time with q measured in $\phi_T = 5 \times 10^{-2}$ pure C_8F_{17} semidilute solutions ($R = 1$) at temperature $T = 30$ °C and for [KBr] = 30 mM.

elongated and flattened particles are available, but it can be speculated that the model meant for polymers is qualitatively valid with possibly different relative amplitudes of the relaxation modes.

The addition of even small amounts (e.g., 10% molar of CTAB) produces a huge drop of the viscosity, suggesting a disruption of the ribbonlike structure and the formation of cylindrical micelles. In our previous study of mixed 12-2-12/CTAB in the presence of 150 mM KBr, it was also shown that the addition of 10% CTAB to a 12-2-12 solution transformed the vesicles into wormlike micelles.[20]

The DLS experiments performed in the solutions of mixed CTAB/C_8F_{17} surfactants with various compositions revealed the same behavior as that obtained in the presence of 200 mM KBr (cf. Figures 7 and 8), that is a bimodal correlation function. The values of $I(q^2=0)$, D_g, A_{fast}, τ_{int}, A_{int}, τ_{slow}, A_{slow}, K_{os}, and of M_g obtained for samples with $\phi = 5 \times 10^{-2}$ at 30 °C and for different values of the molar ratio R are collected in Table 2c. It is important to note that $A_{fast} + A_{int} + A_{slow} = 1$ and that M_g is deduced from eq 15. The most striking observation is the huge decrease of the slow relaxation time when CTAB is added to the solution of C_8F_{17}, as can be observed in Figure 11. This correlates well with the strong increase of fluidity observed visually. At the same time, but to a smaller extent, M_g increases and K_{os} decreases for $R = 1$. All these effects strongly suggest a sharp structural transition. Looking now to the data for the systems with $0.165 < R < 0.9$, it can be seen that τ_{slow} continuously increases with R, suggesting a micellar growth and/or an increase of τ_{break}. Indeed, it can be speculated that the incorporation of C_8F_{17} in the CTAB micelles increases the end-cap energy, thus producing a micellar growth with likely a micellar segregation. Still there is no evidence of intermicellar branching like in the case of compatible surfactants, behavior whose signature is a maximum in the slow relaxation time. The very steep increase of τ_{slow} observed in the vicinity of $R = 1$, as well as the large decrease of K_{os} gives confirmatory evidence of a structural transition within the micellar aggregates. This transition also manifests itself by the appearance in the correlation function of a third relaxation mode with characteristic time intermediate between the collective diffusion time and the reptational time and an amplitude as large as that of the slower mode.

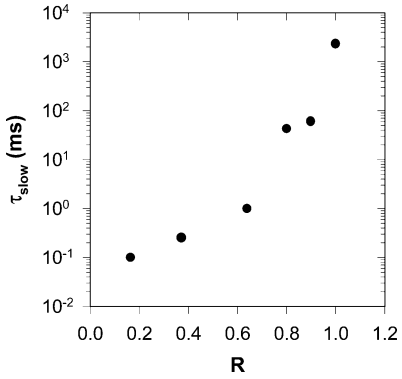

Figure 11. Variation of τ_{slow} with R for $\phi_T = 5 \times 10^{-2}$ semidilute solutions in the presence of 30 mM KBr at $T = 30$ °C.

4. Conclusion

The behavior of mixtures of two surfactants with incompatible fluorocarbon and hydrocarbon hydrophobic moieties has been investigated using light scattering, *T*-jump, and surface tension measurements. The kinetics and dynamical experiments give a self-consistent view of the evolution of the system upon increasing content of the C_8F_{17} surfactant in the mixture and concomitantly the end-cap energy, the two surfactants showing separately a tendency to form self-assemblies with different curvatures. The surface tension measurements performed in the presence of 100 mM KBr suggest the formation in the highly dilute regime of demixed micelles for systems with equimolar composition. In the dilute and semidilute ranges of solutions with 200 mM KBr, the incompatibility of the two surfactants leads to a phase separation at $R = 0.31$ (see partial phase diagram presented in Figure 3). Light scattering and *T*-jump experiments performed on systems with $R < 0.26$ show the presence of a single micelle population with an average micellar length increasing with the C_8F_{17} content. The solutions with 30 mM KBr are monophasic in the whole composition range. The light scattering results strongly suggest a continuous micellar growth upon increasing R without evidence of intermicellar branching as in the case of mixtures of compatible surfactants.

The experimental observations do not allow us to detect a possible micellar demixing. For $R > 0.9$, one observes a huge increase in the viscoelastic relaxation time, which suggests a structural change, in agreement with CryoTEM results showing that the C_8F_{17} forms ribbons instead of cylindrical micelles.

References and Notes

(1) Scamehorn, J. F., Ed. *Phenomena in Mixed Surfactant Systems*; ACS Symposium Series, No. 311; American Chemical Society: Washington DC, 1986.

(2) Holland, P. M., Rubing, D. N., Eds. *Mixed Surfactant Systems*; ACS Symposium Series, No. 501; American Chemical Society: Washington DC, 1992.

(3) Ogino, K., Abe, M. Eds. *Mixed Surfactant Systems*; Surfactant Science Series, Vol. 46; Decker: New York, 1993.

(4) Carlfors, J.; Stilbs, P. *J. Phys. Chem.* **1984**, *88*, 4410.

(5) Asakawa, T.; Hisamatsu, H.; Miyagishi, S. *Langmuir* **1996**, *12*, 1204.

(6) Clapperton, R. M.; Ottewill, R. H.; Ingram, B. T. *Langmuir* **1994**, *10*, 51.

(7) Burkitt, S. J.; Ottewill, R. H.; Hayter, J. B.; Ingram, B. T. *Colloid Polym. Sci.* **1987**, *265*, 628.

(8) Funasaki, N.; Hada, S. *J. Phys. Chem.* **1983**, *87*, 342.

(9) Ghoulam, M. B.; Moatadid, N.; Graciaa, A.; Marion, G.; Lachaise *Langmuir* **1996**, *12*, 5048.

(10) Berr, S. S.; Jones, R. R. M. *J. Phys. Chem.* **1989**, *93*, 2555.

(11) Funasaki, N.; Hada, S. *J. Colloid Interface Sci.* **1980**, *73*, 425.

(12) Asakawa, T.; Miyagishi, S.; Nishida, M. *Langmuir* **1987**, *3*, 821.

(13) Funasaki, N.; Hada, S. *J. Phys. Chem.* **1980**, *84*, 736.

(14) Stähler, K.; Selb, J.; Candau, F. *Langmuir* **1999**, *15*, 7565.

(15) Stähler, K.; Selb, J.; Candau, F. *Colloid Polym. Sci.* **1998**, *276*, 860.

(16) Srinivasa Raghavan, R.; Fritz, G.; Kaler, E. W. *Langmuir* **2002**, *18*, 3797.

(17) Iampietro, D. J.; Kaler, E. W. *Langmuir* **1999**, *15*, 8590.

(18) Zhao, J.; Christian, S. D.; Fung, B. M. *J. Phys. Chem. B* **1998**, *102*, 7613.

(19) Zana, R.; Talmon, Y. *Nature* **1993**, *362*, 228.

(20) Oelschlaeger, C.; Buhler, E.; Waton, G.; Candau, S. J. *Eur. Phys. J. E* **2003**, *11*, 7−20.

(21) Oelschlaeger, C.; Waton, G.; Buhler, E.; Candau, S. J.; Cates, M. E. *Langmuir* **2002**, *18*, 3076.

(22) Oelschlaeger, C.; Waton, G.; Candau, S. J.; Cates, M. E. *Langmuir* **2002**, *18*, 7265.

(23) Faetibold, E.; Waton, G. *Langmuir* **1995**, *11*, 1972.

(24) Esquenet, C.; Buhler, E. *Macromolecules* **2001**, *34*, 5287.

(25) Cummins, H. Z., Pike, E. R., Eds. *Photon Correlation and Light Beating Spectroscopy*; Plenum Press: New York, 1974.

(26) Koppel, D. E. *J. Chem. Phys.* **1972**, *57*, 4814.

(27) Provencher, S. W. *Makromol. Chem.* **1985**, *82*, 632.

(28) Rubingh, D. N. In *Solution Chemistry of Surfactants*; Mittal, K. L. Ed.; Plenum Press: New York, 1979; Vol. 1.

(29) Zana, R.; Lévy, H.; Kwetkat, K. *J. Colloid Interface Sci.* **1998**, *197*, 370.

(30) Alargova, R. G.; Kochijashky, I. I.; Sierra, M. L.; Kwetkat, K.; Zana, R. *J. Colloid Interface Sci.* **2001**, *235*, 119.

(31) Funasaki, N.; Hada, S. *J. Phys. Chem.* **1979**, *83*, 2471.

(32) Asakawa, T.; Hisamatsu, H.; Miyagishi, S. *Langmuir* **1995**, *11*, 478.

(33) Asakawa, T.; Fukita, T.; Miyagishi, S. *Langmuir* **1991**, *7*, 2112.

(34) Israelachvili, J. N.; Mitchell, D.; Ninham, B. *J. Chem. Soc., Faraday Trans. 2* **1976**, *72*, 1525.

(35) Mukerjee, P. *J. Phys. Chem.* **1972**, *76*, 565.

(36) Candau, S. J.; Hirsch, E.; Zana, R. In *Physics of Complex and Supramolecular Fluids*; Safran, S., Clark, N., Eds.; Wiley: New York, 1987.

(37) Adam, M.; Delsanti, M. *Macromolecules* **1985**, *18*, 1760.

(38) Buhler, E.; Munch, J. P.; Candau, S. J. *J. Phys. II* **1995**, *5*, 765.

(39) Nemoto, N.; Kuwahara, M.; Yao, M.; Osaki, K. *Langmuir* **1995**, *11*, 30.

(40) Buhler, E.; Munch, J. P.; Candau, S. J. *Europhys. Lett.* **1996**, *34*, 251.

(41) Brochard, F.; de Gennes, P. G. *Macromolecules* **1977**, *10*, 1157.

(42) Brochard, F. *J. Phys. (Paris)* **1983**, *44*, 39.

(43) Semenov, A. N. *Physica A* **1990**, *166*, 263.

(44) Doi, M.; Onuki, A. *J. Phys. II* **1992**, *2*, 1631.

(45) Wang, C. H. *Macromolecules* **1992**, *25*, 1524.

(46) Cates, M. E. *J. Phys. (Paris)* **1988**, *49*, 1593.

(47) Cates, M. E. *Macromolecules* **1987**, *20*, 2289.

(48) Oelschlaeger, C. Etude des Propriétés Dynamiques de Solutions Micellaires de Tensioactifs Fluorés et Hydrogénés et de leurs Mélanges. Ph.D. Thesis, Louis Pasteur University of Strasbourg, France, 2003.